

condition, in that $-h + k + l = 3n$. Since the electron beam was parallel to the c axis, only $l = 0$ reflections were obtained, and only the a_0 parameter could be determined. Nevertheless, the agreement on the a_0 parameter and the silvery white appearance of the material leave little doubt that the coating on the graphite is the same substance as that found in the graphitic gneiss from the Ries Crater (1). However, conditions of formation here indicate that it is very unlikely that this white allotropic form of carbon is a high-pressure form as was originally inferred. Indeed the conditions under which we produced the new form of carbon were low pressure and high temperature.

There were reflections in the diffraction pattern that did not fit the hexagonal array. Some of these were measured and were found to form a rectangular pattern and the d values correspond to α SiC form I (4). This indicates that the electron beam was normal to an a axis of SiC to give only $k = 0$ reflections and implies that the SiC crystals had a fixed orientation to either the white carbon crystals or the graphite basal planes. The white carbon contained about five times as much silicon as the natural material described by El Goresy and Donnay (1). This had no measurable effect on the a_0 parameter; hence, it is unlikely that the silicon is directly involved in the white carbon phase. Silicon may act as a flux for the formation of the white carbon; however, additional experiments showed that white carbon can be just as easily synthesized in a silicon-free system.

The white carbon coating is a transparent birefringent material; therefore, its white appearance is due to light scattered by the large number of surfaces. Also, the extinction behavior agreed with the observation that all the dendrites had the same crystallographic orientation, and with the implication that they grew perpendicular to the edges of the basal planes with an a axis parallel to the planes. Unfortunately, no index of refraction data could be obtained because the crystals were much too small.

In an article entitled "Dendrites of graphite" (5) four figures show dendritic growth identical to that which we observe in the new phase of carbon. It thus appears likely that this new phase, which often appears as a transparent coating on graphitic crystals, may have been missed repeatedly in the past.

Note added in proof: Twenty-three additional d values which were ob-

tained from several small randomly oriented white carbon crystals were used to calculate the unit cell dimensions: $a_0 = 8.945 \pm 0.007$ Å, $c_0 = 14.071 \pm 0.011$ Å.

A. GREENVILLE WHITTAKER
P. L. KINTNER

Materials Sciences Laboratory,
Aerospace Corporation,
El Segundo, California

References and Notes

1. A. El Goresy and G. Donnay, *Science* **161**, 363 (1968).
2. A. G. Whittaker and P. Kintner, *Carbon*, in press.
3. The scanning electron microscope was a Cambridge Stereoscan Mark 2 operated at 20 kv with a spot diameter of ~ 100 Å; the

electron microprobe was an Applied Research Laboratories model EMX with a beam diameter of ~ 0.5 μ at ~ 4 μ penetration; the electron microscope used for the electron diffraction work was a Jeolco model 5 G with a beam diameter of ~ 2 μ and a beam energy of 80 kv.

4. N. W. Thibault, *Amer. Mineral.* **29**, 327 (1944).
5. I. Nakoda and Y. Tamai, in SM-68016 Applications of the Japan Electron Optics Laboratory Scanning Electron Microscope (Jeolco, Ltd., Medford, Massachusetts), p. 11.
6. We thank H. Parish and J. Dancy (Naval Weapons Center, China Lake, California) for scanning electron microscopy and electron diffraction work, respectively; G. M. Wolten and J. H. Richardson (Aerospace Corporation) for assistance in interpretation of the electron diffraction pattern and photography, respectively; and J. Ogren and R. Commingham (Autonetics, North American Rockwell Corporation, Anaheim, California) for electron microprobe analysis.

28 May 1969

Enstatite: Disorder Produced by a Megabar Shock Event

Abstract. Shocked Bamle enstatite partly transforms to disordered enstatite. Debye-Scherrer patterns of some shocked material are almost identical to those of disordered enstatite from portions of various enstatite achondrites. No disordered single crystals have been found.

Disordered enstatite (1), which was first found in 1963 (2) in Cumberland Falls and Norton County achondrites, was subsequently found in all the enstatite achondrites except those from Shallowater (3). The presence of disordered enstatite was also noted in five enstatite chondrites, 20 ordinary chondrites, and in synthetic samples cooled fairly rapidly from 2800°C (4). Since the enstatite achondrites, except Shallowater, are highly brecciated, one possible origin of the disordered enstatite is shock deformation. Samples of enstatite from Bamle, Norway, shocked at 150 to 200 and 400 to 450 kb did not show evidence of disordered

enstatite (4). We now report the observation of disordered enstatite in samples shocked to pressures of approximately 1 Mb.

Disks of Bamle enstatite, ~ 19 mm in diameter by 2.5 mm thick, were fitted into stainless steel sample capsules, which in turn were fitted into holes in a steel block surrounded by steel spall plates. The capsule assemblies were impacted by a stainless steel disk (3 mm thick) which had been explosively accelerated to a velocity of 3.6 to 3.7 km/sec. Peak shock pressures in the samples were in the range of 0.9 to 1.0 Mb, and the duration of the pressure pulse was less than 1 μ sec.

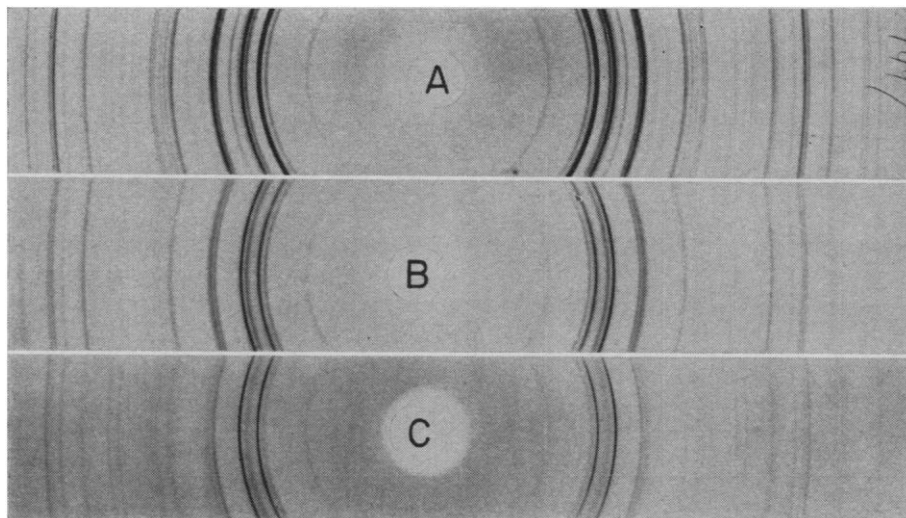


Fig. 1. Debye-Scherrer photographs of ordered enstatite from Khor Temiki enstatite achondrite (A); disordered enstatite from Aubres enstatite achondrite (B); and disordered enstatite from Bamle enstatite shocked at 1 Mb (C).

Specimen temperatures on release of shock pressure were estimated to be 500° to 1400°C.

Most of the small crystals chosen for examination from the shock-loaded sample transmit light, but single-crystal x-ray photographs show that they are highly mosaic enstatite. Approximately 20 single crystals from samples shocked at a pressure of 1 Mb have been examined by single-crystal x-ray techniques, and none showed the alternating sharp and diffuse spot patterns (4) produced by disordered enstatite. A Debye-Scherrer pattern made

of a randomly selected sample resembles a mixture of ordered and disordered enstatite; therefore, it is likely that a white powder coating the crystals is disordered enstatite. Some white opaque grains approximately 0.2 mm on edge, which give Debye-Scherrer patterns (Fig. 1) almost identical to those of disordered enstatite from enstatite achondrites, have also been isolated from the sample. Table 1 lists the *d* spacings and intensities of ordered enstatite from Bamle, Norway, disordered enstatite from the Cumberland Falls achondrite, and disordered enstatite produced by a megabar shock event. Disordered enstatite single crystals from enstatite achondrites contain a small amount of twinned clinoenstatite. Thus far we have found no evidence of twinned clinoenstatite in artificially shocked enstatite, but we cannot rule out the possibility that it is present.

In our shock pressure and temperature calculations we have assumed that the Hugoniot equation of state for Bamle enstatite corresponds approximately to the Hugoniot equations reported by McQueen *et al.* for Bushveld and Stillwater bronzites (5). The pressure estimates are insensitive to large deviations from the assumed Hugoniot equation. The postshock temperature estimates, however, are quite sensitive to both the Hugoniot equation and to the release adiabat, that is, the path followed by the material (in the pressure-volume plane) on release of pressure. The large uncertainty in the estimated postshock specimen temperature is the result of calculations of the limits of possible values and primarily reflects the lack of any experimental data on the release adiabat for pyroxenes.

At present, we are unable to determine whether the disordered enstatite found in the shock-loaded samples resulted from high shock pressures, from high postshock temperatures, or perhaps from the combination of the two. We cannot exclude the possibility that the enstatite samples were at sufficiently high temperature on release of pressure to be in the protoenstatite stability field (6) and that the disorder could have been more easily produced by a simple thermal cycle.

Additional evidence indicates that many meteorites, both irons and stones, have experienced shock pressures of about a megabar (7). We suggest that most occurrences of disor-

dered orthopyroxene in enstatite and eucrite achondrites can be interpreted as the result of high shock pressures, but we would emphasize that the presence of disordered orthopyroxene in meteorites, especially chondrites (8), is not unequivocal evidence of shock damage.

SIDNEY S. POLLACK

Mellon Institute,
Carnegie-Mellon University,
Pittsburgh, Pennsylvania 15213

PAUL S. DECARLI

Stanford Research Institute,
Menlo Park, California 94025

References and Notes

1. The term "disorder" has been used to describe two different structural aspects of pyroxenes: (i) stacking and (ii) Mg-Fe disorder. Here it refers to stacking disorder.
2. W. L. Brown and J. V. Smith, *Z. Kristallogr.* **118**, 186 (1963).
3. S. S. Pollack, *Amer. Mineral.* **51**, 1722 (1966).
4. ———, *Geochim. Cosmochim. Acta* **32**, 1209 (1968).
5. R. G. McQueen, S. P. Marsh, J. N. Fritz, *J. Geophys. Res.* **72**, 4999 (1967).
6. F. R. Boyd and J. L. England, *Carnegie Inst. Wash. Year B.* **64**, 117 (1964-65).
7. K. Fredriksson, P. S. DeCarli, A. Aaramac, *Space Res.* **3**, 974 (1963); D. Heymann, M. E. Lipschutz, B. Nielsen, E. Anders, *J. Geophys. Res.* **71**, 619 (1966); N. L. Carter, C. B. Raleigh, P. S. DeCarli, *ibid.* **73**, 5439 (1968).
8. Bjurböle and Chainpur are examples of chondrites in which the disordered orthopyroxene is probably not due to shock effects.
9. S. S. Pollack and W. D. Ruble, *Amer. Mineral.* **49**, 983 (1964).
10. Supported by NASA grant No. NGR 39-008-013.

24 March 1969; revised 12 May 1969

Macrophage Ribonucleoprotein: Nature of the Antigenic Fragment

Abstract. *The antigenic fragments of bacteriophage T2 recovered in RNA derived from macrophages infected with T2 bacteriophage retain their capacity to combine with specific neutralizing antibody to T2. The preservation of the complete native tertiary structure of tail fiber antigen of bacteriophage T2 is not required for immunogenicity.*

An unusual ribonucleoprotein of macrophages has the ability to combine with antigens to which these cells are exposed. This antigen-ribonucleoprotein complex can induce the production of specific antibody against the challenging antigens (1, 2). Some features of this complex of antigen and ribonucleoprotein (RNP) are a unique density in cesium sulfate solution (1.588 g/cm³), a protein content of 28 percent, and an approximate molecular weight of 12,000 (3). These facts indicate that the maximum size of the antigenic frag-

Table 1. Intensity data for ordered Bamle enstatite, disordered Cumberland Falls enstatite, and Bamle enstatite shocked at 1 Mb; CuK α_1 radiation; wavelength = 1.5405 Å; U, lines from minerals other than enstatite; W, weak lines seen easier on photographs; B, broad lines.

Bamle*		Cumberland Falls*		Shocked Bamle†	
<i>d</i> (Å)	<i>I</i> / <i>I</i> ₁	<i>d</i> (Å)	<i>I</i> / <i>I</i> ₁	<i>d</i> (Å)	<i>I</i> / <i>I</i> ₁
6.33	< 1	6.3	W	6.4	3
4.43	3	4.41	8	4.44	7
4.028	1		W		
3.314	6	3.30	15	3.29	18
U 3.233	1				
3.175	100	3.17	84	3.18	84
U 3.122	2				
U 3.049	5	2.96	28	3.00	33
		2.94			
2.946	16	2.87	100	2.88	100
2.878	54	2.82	W		
2.832	9				
U 2.746	2				
2.710	10	2.70	W, B		
2.540	25	2.53	26	2.56	20
2.497	18	2.49	39	2.48	29
		2.47			
2.477	18				
U 2.386	< 1	2.36	W, B		
2.364	1				
U 2.320	< 1				
2.283	1	2.28	3		
2.257	3	2.24	W		
2.239	3	2.22	W, B		
2.116	12	2.11	21	2.12	20
		2.09			
2.100	12	2.05	10	2.03	23
2.060	5	2.01			
2.025	7	1.98	7	1.99	20
1.988	9				
1.961	11	1.92	W		
1.929	1				
1.888	4	1.85	W, B		
1.841	4				
1.803	1				
1.788	4	1.78	11	1.79	25
1.779	3	1.77	W, B		
1.737	6	1.73	6	1.74	16
1.710	6				
1.681	1	1.67	W, B	1.67	5
1.652	1	1.64	W, B	1.62	18
1.610	11	1.60	14		
1.591	6	1.58	7		
1.529	5	1.53	15	1.53	24
		1.52			
1.522	7	1.49	12	1.49	10
1.488	23	1.47	21	1.47	30
1.473	17				

* Data from Pollack and Ruble (9). † Intensities determined from densitometer trace of Fig. 1C.